Available online at www.sciencedirect.com
ScienceDirect
Food Chemistry 105 (2007) 400–404
Food Chemistry
www.elsevier.com/locate/foodchem

Compositional and structural investigations of ripening of table olives, *Bella della Daunia*, by means of traditional and magnetic resonance imaging analyses

Maria Antonietta Brescia [a], Tonietta Pugliese [a], Edme Hardy [b], Antonio Sacco [a,*]

[a] *Dipartimento di Chimica, Campus Universitario, Università di Bari, Via Orabona 4, 70126 Bari, Italy*
[b] *Institut für Mechanische Verfahrenstechnik und Mechanik, Universität Karlsruhe, 76128 Karlsruhe, Germany*

Received 3 October 2006; received in revised form 2 December 2006; accepted 17 December 2006

Abstract

The ripening of *Bella della Daunia* table olives was monitored and the structural and compositional differences between the raw and processed products were investigated. The amount of oil in the pulp, the moisture, the reducing sugar content and the composition of fatty acids were determined by means of routine analyses. The results provided information on the variations that occur in the *Bella della Daunia* olive with ripening. They confirmed the correlation between decreases in sugars and water and increases in oil content. Analyses carried out on processed olives showed the effects of processing on components.

Magnetic resonance imaging (MRI) was employed in order to monitor (non-invasively) the different stages of maturation and the processed olives. This technique proved useful for monitoring the evolution of water and oil distribution.

Keywords: Table olives; Ripening; Oil; Reducing sugars; Fatty acids; Magnetic resonance imaging

1. Introduction

Bella della Daunia table olives were awarded *Protected Designation of Origin* (PDO) status in 2000 (European Communities, 2000), in accordance with community regulation 2081/92. PDO is awarded to typical agricultural foods whose characteristic features are fundamentally or exclusively due to geographical environment, including both natural and human factors; besides, production, transformation and processing must occur in the place of origin according to the corresponding production disciplinary (European Communities, 1999). *Bella della Daunia* table olives are produced in a restricted area in the province of Foggia, Apulia (Southern Italy). Environmental factors, together with the variety and the methods of cultivation, harvesting and processing, define the typical and organoleptic features of the olive, regarded as one of the best cultivars for the production of table olives. The purpose of this study was to investigate the changes of a number of compounds found in *Bella della Daunia* olives during ripening and after processing. To this end, the amount of oil in the pulp, the moisture and reducing sugar content, and the composition of fatty acids were determined. While the literature has extensive data on the composition of olives during ripening (Nergiz & Engez, 2000; Rial & Falqué, 2003; Finotti et al., 2001), there is no information on the structural distribution of oil and water in olive tissue, nor on the changes taking place due to ripening and processing. Magnetic resonance imaging (MRI) enables the quality and ripening-related processes in agricultural products to be monitored non-invasively (Clark, Hockings, Joyce, & Mazucco, 1997; Jagannathan, Govindaraju, & Raghunathan, 1995; Joyce, Hockings, Mazucco, & Shorter, 2002; Gussoni et al., 1993). Since olive fruit has a high oil content

* Corresponding author. Tel.: +39 080 5442042; fax: +39 080 5442129.
E-mail address: antonio.sacco@chimica.uniba.it (A. Sacco).

0308-8146/$ - see front matter © 2007 Elsevier Ltd. All rights reserved.
doi:10.1016/j.foodchem.2006.12.027

with a resonance signal from oil protons that resonates about 3.5 ppm away from water, chemical shift selective MRI experiments could be carried out in order to identify oil and water distribution separately and to estimate the variations as ripening progressed.

The objective of combining traditional and MRI analyses is to obtain a complete chemical and structural study of olive ripening.

2. Materials and methods

2.1. Olive samples

Sufficient amounts of olives were hand-picked from all sides of one olive tree from October 2002 to January 2003. The samples analysed are shown in Table 1. Sample 6 was made up of pickled green olives processed by the Sivigliian method, while sample 7 was made up of pickled black olives, processed using the Californian system.

The samples were immersed in liquid nitrogen, and stored at −80 °C prior to analysis.

2.2. Moisture, oil, fatty acids and reducing sugars determinations

Moisture content was determined by measuring the weight difference when 10 g of homogenised olives were dried in an oven at 105 °C for 5 h.

Oil content was determined by Soxhlet extraction, using petroleum ether on homogenised olives dried in an oven at 50 °C.

Fatty acid composition was determined by gas chromatography (GC), using previously described procedures and instrumentation (Sacco et al., 2000).

Reducing sugars were twice extracted from 1 g of homogenised freeze-dried olives with 20 ml of water–ethanol solution (1:1) for 30 min. The extracts were filtered using a funnel with fritted glass filter support and evaporated at 40 °C to eliminate the ethanol. The solution was brought to 100 ml with water. This solution was used to titrate the Fehling solution (1 ml of reagent A: copper sulphate, 1 ml of reagent B: sodium and potassium tartrate and NaOH, 15 ml of water), using methylene violet as indicator.

Table 1
List of the analysed samples

Sample number	Picking date
1	30/10/02
2	11/11/02
3	27/11/02
4	18/12/02
5	13/01/03
6	Green pickled olives
7	Black pickled olives

2.3. MRI measurements

The imaging experiments were performed at 4.7 T (200 MHz for ^{1}H) on a Bruker Avance 200SWB NMR spectrometer operated with PARAVISION. The Micro2.5 gradient system has an inner diameter of 40 mm and produces maximum gradients of 1 T/m. The radio-frequency birdcage resonator has an inner diameter of 25 mm, restricting the sample diameter to about 23 mm. A spin-echo imaging sequence, with a chemical shift selective excitation pulse and a slice-selective refocusing pulse, was used to obtain selective images. The field of view of 25 mm × 25 mm was divided into 128 × 128 voxels; the repetition time was 2 s and the echo time 8.2 ms.

Images of the three olives were obtained using the Mini0.36 gradient system with an internal diameter of 85 mm and maximum gradients of 0.14 T/m. The corresponding birdcage resonator had an inner diameter of 64 mm.

3. Results and discussion

3.1. Routine analyses

Fig. 1 shows moisture, oil and reducing sugar contents for the samples. The decreasing moisture content during ripening is typical of olives of other cultivars (Nergiz & Engez, 2000). The moisture content is due to biological development, but also to human and climatic factors, such as irrigation, rainfall and temperature. The high moisture content of sample 5 compared to sample 4 can probably be attributed to picking after rainfall or irrigation.

The amount of oil increased over the course of the sampling period, while reducing sugar content decreased, except for the last sample. A relationship was found between oil accumulation and sugar content. This correlation can be explained by considering that sugars are precursors of fatty acid biosynthesis in the olive fruit (Wodner, Lavee, & Epstein, 1988).

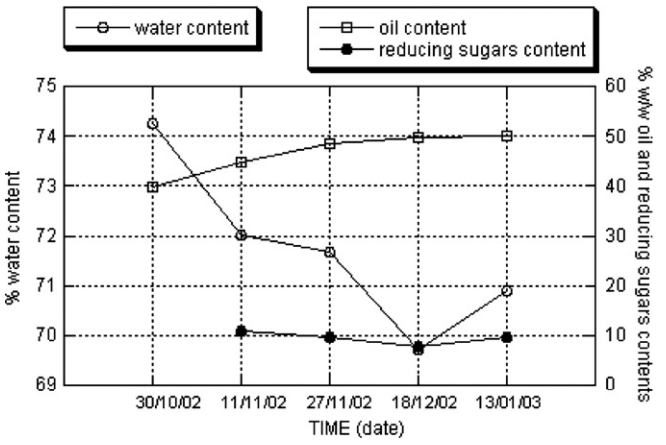

Fig. 1. Moisture, oil, and reducing sugars contents of the analysed olives.

Water contents in samples 6 and 7 were higher than those in the other samples, probably because of the washings they undergo during processing; in fact, the osmotic process raises the water content of olive tissue (Bianchi, 2003; Marsilio, Campestre, & Lanza, 2001). The oil content of these samples was unchanged, while reducing sugar content decreased, probably due to being solubilized in washing water.

Table 2 shows the percentage content of fatty acids. The most common fatty acids in these olives were oleic, palmitic, linoleic, stearic and behenic acid. Fatty acid content does not present any particular trend with ripening; however, it is noticeable that, with ripening, the oil fraction sensibly enriches in longer-chain fatty acids. Samples 6 and 7 have the same fatty acid composition as the other samples, showing that processing does not influence oil composition.

3.2. MRI analysis

The olive is structurally constituted of different parts: the epicarp, the mesocarp and the endocarp. The latter contains the seed, made up of the tegument, the albumen and the embryo (Fig. 2).

The chemical shift selective MRI images for samples 2, 3 and 5 are shown in Fig. 3 (sample 5 had to be slightly cut in order to fit into the resonator). Image 3a shows water presence in the pulp near the epicarp, but also around the endocarp, with a radial crown distribution. The signal intensities show that the water quantities near the epicarp and the endocarp are comparable. Water is also present in the seed, but in a minor quantity. A detailed analysis of image 3a shows that there is more water in the tegument and in the embryo than in the albumen.

The oil selective image (3b) presents a less evident distribution. Oil is located principally around the endocarp and becomes less abundant toward the mesocarp, again with a radial crown distribution. The seed has a well-defined oil distribution, with oil appearing to be concentrated in the centre of the embryo. Moreover, the intensity of the oil signal in the seed is higher than that in the pulp.

Table 2
Fatty acids [%] of oil extracted from the analysed olives

Fatty acids	Sample 1	Sample 2	Sample 3	Sample 4	Sample 5	Sample 6	Sample 7
C14:0	0	0	0	0.28	0.22	0	1.04
C16:0	17.1	18.8	16.3	18.9	19.4	15.5	18.3
C16:1	0.96	0.93	0.56	0.57	0.64	0.73	0.33
C17:1	0	0.21	0	6.63	0	0	0
C18:0	3.60	3.95	4.09	4.25	5.10	3.48	3.87
C18:1	62.3	60.8	62.4	54.9	57.8	68.2	54.5
C18:2	7.81	9.22	8.37	7.22	8.86	9.44	6.20
C20:0	0	0.90	0	0.22	0	0	0
C18:3	0.65	0.47	0.61	0.60	0.54	0	0.87
C20:1	1.09	0.42	0.78	0.51	0.77	0.79	0
C22:0	3.01	2.10	3.68	5.01	3.93	1.08	3.56
C24:1	1.86	0.98	2.23	0. 0	1.13	0.77	1.63
C22:6	0.60	0.38	0.47	0.47	0.47	0	9.29

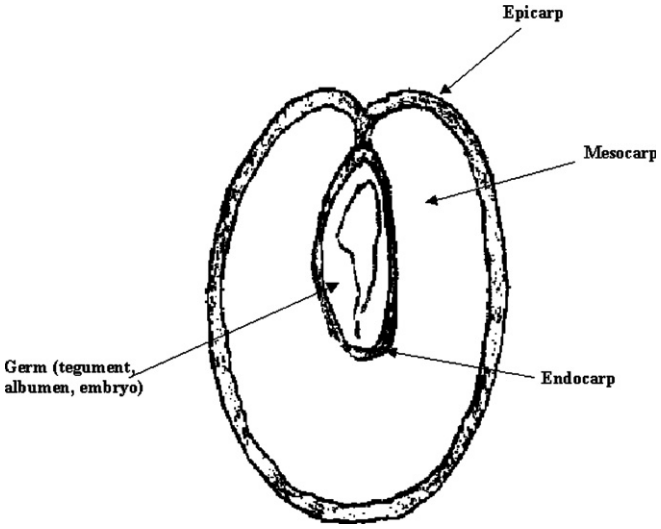

Fig. 2. Olive section.

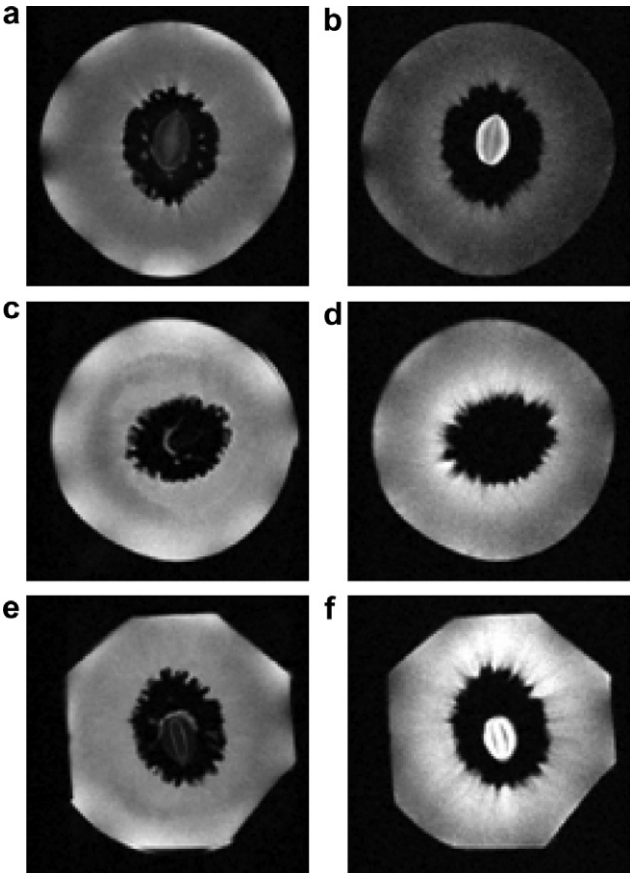

Fig. 3. Axial images of olives. (a) Water selective image and (b) oil selective image of sample 2; (c) water selective image and (d) oil selective image of sample 3; (e) water selective image and (f) oil selective image of sample 5.

Image 3c shows the distribution of water in the olive in sample 3. It is comparable to that observed in sample 2, but the radial crown distribution around the endocarp is not evident. Water is concentrated in the outer pulp. This could indicate the water trend with ripening.

The oil distribution observed in image 3d is analogous to that of sample 2. From a comparison of the signal intensities, it seems evident that oil is concentrated near the endocarp. In this image, the germ signal is absent, which is surprising, since it is known that the germ contains a certain quantity of oil. This result has been investigated more accurately in further experiments and will be discussed later.

The characteristics of images 3e and f are analogous to those of sample 3, except for the fact that the seed is evident and assumes the same structural characteristics as sample 2. Moreover, image 3e has a sufficiently high resolution to show that the distribution of water in the embryo is not uniform. Intensity comparison shows that the water content in the seed from sample 5 is lower than that in the one from sample 2, while oil content increases and is more homogeneously distributed in the pulp, in agreement with previous studies (Gussoni et al., 1993). This trend is consistent with the observation that water content, both in the seed and in the pulp, is reduced.

The images of the processed products are shown in Fig. 4. In the water selective image 4a the water signal is almost completely located in the entire mesocarp region and in a thin layer around the epicarp, while its intensity decreases towards the endocarp. Particularly, in this image, there are alternating bright and dark areas close to the epicarp. These areas are close to the rods of the birdcage resonator and show artifacts due to inhomogeneities in the radio-frequency field. The seed structure is not evident but there is a water-rich region in its lower right corner. In the oil selective image, the signal intensity is higher around the endocarp and decreases toward the flesh. The distribution of oil in the seed is the same as in the previous samples.

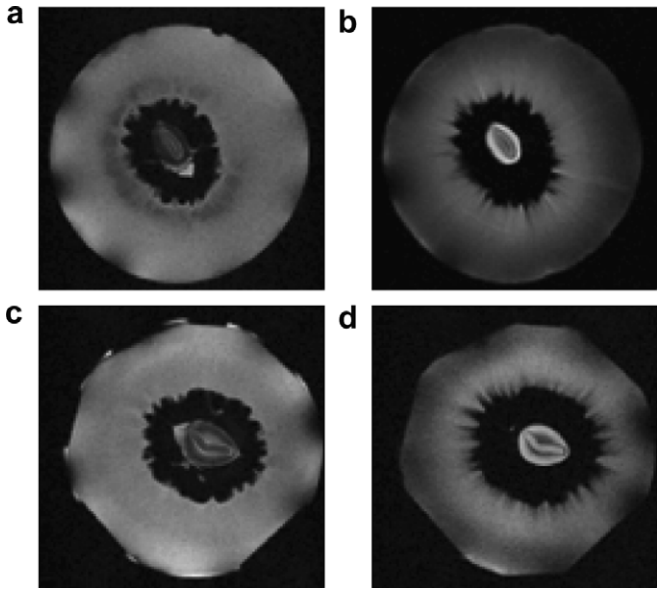

Fig. 4. Axial images of processed olives. (a) Water selective image and (b) oil selective image of green pickled olives (sample 6); (c) water selective image and (d) oil selective image of black pickled olives (sample 7).

These images introduce a few considerations. First, in raw olives, water and oil are both concentrated around the endocarp. A tentative explanation for this behaviour, assuming that there is a high porosity region around the endocarp, is that both water and fat will concentrate in this area, resulting in an undifferentiated distribution of these two components in the pulp.

During ripening, water seems to move from the inner mesocarp toward the outer mesocarp. To explain this phenomenon, some authors have considered (Joyce et al., 2002) that, with ripening, an increase in permeability or the rupture of a cell membrane could lead to the displacement of air. For this reason, signals due to water protons, that were previously adjacent to spaces occupied by air, are no longer dephased and give a stronger signal.

One of the most relevant questions emerging from this study regards the absence of the seed signal in the oil selective image. This was observed on one olive picked on 27/11/02 (Fig. 3d) and one on 13/01/02 (images not shown). This is not easily explainable, since it is known that the seed contains both water and oil at the same time. The signal was also not visible using volume-selective spectroscopy. To finally ascertain this result, a simple one-pulse spectrum from the entire isolated kernel was recorded, and still there was no signal about 3.5 ppm downfield from water. For this reason, it was supposed that the oil components of the seed are supported on woody constituents of the seed, thus losing mobility and relaxing too fast to give narrow signals. In contrast with previously reported data (Gussoni et al., 1993), this phenomenon does not seem to be dependent on ripening.

In order to study the differences between fruits picked on the same day, and to evaluate whether the observations performed on the samples can be generalised, three olives picked on 27/11/02 were inserted into a gradient system with a 64 mm internal probe diameter. The images obtained are shown in Fig. 5.

Although there are no evident differences in the water selective image, in the oil selective image, the top olive does not show the band of high intensity around the seed that is present in the other two olives. This leads to the conclusion that ripening in the different fruits can occur at different times and the factor that influences this behaviour may

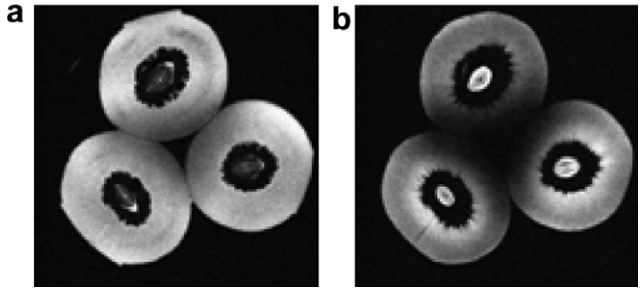

Fig. 5. Axial images of three olives. (a) Water selective image and (b) oil selective image of sample 3.

be a different position on the tree. This suggests that it is not possible to generalise our considerations, unless MRI investigations are carried out on a large number of different fruits picked on the same day. Also evident in Fig. 5, is a darkened region around the air/olive interface in the centre of the picture, again showing a susceptibility artefact. This artefact will be studied carefully if quantitative analysis is performed.

4. Conclusions

The results provide information on the variations that occur in the *Bella della Daunia* olive with ripening. They confirm the correlation between decreases in sugars and water and increases in oil content. Routine analyses carried out on processed olives showed how processing affects components.

MRI highlighted local movements of macro-components in the pulp during ripening. Evidence was obtained of a wave of apparent high water activity moving out from the inner to the outer mesocarp during the ripening process.

The questions arising from this work (absence of the oil signal in some seeds and differences between olives picked on the same day) warrant extended work on a larger number of olives picked in different years in order to show the relationship between these behaviours and the degree of ripening.

The MRI approach could be used to characterize olives of different cultivars to provide information about the NMR parameters that differentiate the olives and explain characteristics such as pulp consistency and detachment of the pulp from the kernel.

The results of such a study should be of value in the agricultural industry for quality control and for characterizing typical agricultural products.

Acknowledgements

We thank the "La Bella di Cerignola" co-operative for supplying us with the olive samples. We also acknowledge Emilio Oliver-Gonzalez, Domenico Benedetti and Giovanna Alviti for their technical support, Manfred Holz for his helpful comments, and Anthony Green for proofreading and providing valuable linguistic advice.

References

Bianchi, G. (2003). Lipids and phenols in table olives. *European Journal of Lipid Science and Technology, 105*, 229–242.

Clark, C. J., Hockings, P. D., Joyce, D. C., & Mazucco, R. A. (1997). Application of magnetic resonance imaging to pre- and post-harvest studies of fruits and vegetables. *Postharvest Biology and Technology, 11*, 1–21.

European Communities (1999). Application 2/99, Official Journal of the European Communities, C358.

European Communities (2000). Regulation 1904/00, Official Journal of the European Communities, L228.

Finotti, E., Beye, C., Nardo, N., Quaglia, C. B., Milin, C., & Giacometti, G. (2001). Physico-chemical characteristics of olives and olive oil from two mono-cultivars during various ripening phases. *Nahrung/Food, 45*, 350–352.

Gussoni, M., Greco, F., Consonni, R., Molinari, H., Zannoni, G., Bianchi, G., et al. (1993). Application of NMR microscopy to the histochemistry study of olives (*Olea europea* L.). *Magnetic Resonance Imaging, 11*, 259–268.

Jagannathan, N. R., Govindaraju, V., & Raghunathan, P. (1995). In vivo magnetic resonance study of the histochemistry of coconut (*Cocos nucifera*). *Magnetic Resonance Imaging, 13*, 885–892.

Joyce, D. C., Hockings, P. D., Mazucco, R. A., & Shorter, A. J. (2002). ^{1}H Nuclear magnetic resonance imaging of ripening "Kensington pride" mango fruit. *Functional Plant Biology, 29*, 873–879.

Marsilio, V., Campestre, C., & Lanza, B. (2001). Sugar and polyol compositions of some European olive fruit varieties (*Olea europea* L.) suitable for table olive purposes. *Food Chemistry, 74*, 55–60.

Nergiz, C., & Engez, Y. (2000). Compositional variation of olive fruit during ripening. *Food Chemistry, 69*, 55–59.

Rial, D. J., & Falqué, E. (2003). Characteristics of olive fruits and extra-virgin olive oils obtained from olive trees growing in appellation of controlled origin 'Sierra Mágina'. *Journal of the Science of Food and Agriculture, 83*, 912–919.

Sacco, A., Brescia, M. A., Liuzzi, V., Reniero, F., Guillou, C., Ghelli, S., et al. (2000). Characterization of the geographical origin and variety of Italian extra virgin olive oils based on analytical and NMR determinations. *Journal of the American Oil Chemists' Society, 77*, 619–625.

Wodner, M., Lavee, S., & Epstein, E. (1988). Identification and seasonal changes of glucose, fructose and mannitol in relation to oil accumulation during fruit development in *Olea europaea* (L). *Scientia Horticulturae, 36*, 47–54.